# State Feedback Predictive Control for Non-linear Hydro-turbine Governing System

Yapeng Yi[1], Zhiwang Zhang[1], Diyi Chen[1,2*], Rui Zhou[1], Edoardo Patelli[3], Silvia Tolo[3]

[1]*Institute of Water Resources and Hydropower Research, Northwest A&F University, Shaanxi Yangling 712100, China*

[2] *Australasian Joint Research Centre for Building Information Modelling, School of Built Environment, Curtin University, WA, 6102, Australia*

[3]*Institute for Risk and Uncertainty, University of Liverpool, Liverpool, United Kingdom*

**Telephones**: 086-181-6198-0277
**E-mail**: diyichen@nwsuaf.edu.cn

**Abstract:** The present work introduces a novel predictive control strategy for the analysis of the dynamic performance of hydro-turbine governing systems based on fuzzy logic. Firstly, a six-dimensional non-linear dynamic model of the system is defined. The defined model is applied to a realistic case-study, aiming to investigate the dynamic behavior of the system. In order to deal effectively with the non-linearity of the system under study, the T-S fuzzy approach is adopted. The results demonstrated through the use of the discrete Lyapunov function and Schur complements of matrices suggest that the closed-cycle control system can achieve a global asymptotic stability state. The second part focuses on the quantification of the impact of sudden changes in operating conditions on the overall performance. The numerical results indicate that proposed predictive control method can ensure the performance of the system to be reliable and robust to external inferences. In addition to this, the approach proposed has unquestionable advantages over the traditional PID and model predictive controllers with regard to non-linear systems applications.

**Keywords:** State feedback predictive control, T-S fuzzy model, hydro-turbine governing system, non-linear, stability

## 1. Introduction

Hydraulic turbine governing systems (HTGSs) are sophisticated non-linear, multi-input multi-output and non-minimum phase systems, which generally include the turbine, the pressure diversion, the reservoir, the governor, the grid and the load of hydropower systems (Li et al., 2016; Li et al., 2017). However, with the rapid growth of the hydropower installed capacity in the last decades and the subsequent construction of large installations has widened the level of uncertainty affecting the dynamic behavior of HTGSs (Xu et al., 2015). In more detail, the accuracy in the monitoring of these systems is strongly affected by many factors, e.g., the randomness of the load disturbance, the uncertainty related to the non-linear adjustment of the servomotor (Xu et al., 2016; Guo et al., 2015). This high degree of uncertainty and random disturbance have the potential to significantly increase the risks of generator swing and network-disconnecting, it is therefore important to predict the dynamic performance of HTGS. In light of this, implementing a new theoretical and computational tool that is able to fully capture such the uncertainty interference is particularly important (Mahmoud et al., 2005; Donaisky et al., 2015).

During the last decades, traditional algorithms based on the use of a limited number of parameters have been adopted for PID controllers (Martinez-Lucas et al., 2015; Zhang et al., 2015; Zhang et al., 2006; Hao, 2000). However, due to the development of the hydropower industry, the simplified model is not adequately described the uncertainties caused by internal structural parameters of the non-linear systems (Chen et al., 2015). In other words, the theoretical approach behind

traditional control algorithms is not fully adequate to deal with the new challenges that the engineering practice need to face in the field of hydropower. To fill this gap, several predictive control methods have been introduced and are nowadays quite established in the scientific literature (Mobayen et al., 2017; Mobayen, 2014; Cortes et al., 2008; Liu et al., 2016). Such methods aim to provide on-line optimization and feedback correction according to the feedback prediction control models (Zhang et al., 2015; Takacs et al., 2014; Mobayen, 2015). These can solve the problem of parameters uncertainty in the analysis of the high-dimensional complex model, and hence enhance the robustness and anti-interference of the system to random disturbances (Mobayen, 2016; Mobayen et al., 2017; Wang et al., 2016). The research described in this paper focuses on the analysis of the dynamic characteristics of HTGSs adopting a predictive control algorithm and aiming to provide a reliable theoretical background for the safe and stable operation of the hydropower station (Munoz-Hernandez et al., 2015).

The purpose of the study is achieved through the adoption of the Model Predictive Control (MPC) method. It refers to use optimization control algorithms to provide predictions regarding the system behavior, preform rolling optimization and finally feedback corrections on the basis of the dynamic errors obtained (Kishor, 2008; Kim et al., 2008; Munoz-Hernandez et al., 2015; Dutta et al., 2016). Many predictive control algorithms have been implemented an applied in the industrial field in recent years. One of the first examples have been used this kind of method in the Boiler-Turbine industry is the Dynamic Matrix Control (DMC) in Ref (Moon et al.,

2009; Wu et al., 2014). It tackles the output error in the case of steady-state at the cost of a higher computational demand. An alternative to the DMC approach is represented by the Generalized Predictive Control (GPC), adopted in the study by Ref (Zambelli et al., 2012; Errouissi et al., 2016; Tran et al., 2015; Brown et al., 2013). This is a robust adaptive control algorithm but it presents strong limitations in dealing with non-linear systems. To overcome the limitation of previous approaches, the State Feedback Predictive strategy has been proposed: in this kind of algorithms the introduction of a state feedback loop allows to efficiently provide state feedback correction (Zhang et al., 2008; Ji et al., 2009). Furthermore, it is less computational demanding than DMC and GPC approaches and requires only a restrict number of parameters in the model definition. In light of this, the current research focuses on the integration of the state feedback predictive control approach, adopted for the control optimization of non-linear hydraulic turbine systems with the T-S fuzzy model, which provides the modelling of non-linear systems with arbitrary parameters precision (Su et al., 2007; Chen et al., 2013; Lam, 2009; Rastegar et al., 2016).

Inspired by what has been discussed above, there are four innovations of this paper which make the proposed method more appealing compared with previous works. This study firstly consists of the definition of a six-dimensional nonlinear dynamic model for the HTGS, which provides an accurate representation of real systems. The second innovation is the state feedback predictive control of HTGS applied in T-S fuzzy model, which makes the global output of the HTGS model have good mathematical expression characteristics. Thirdly, the SFPC that has both output

feedback and state feedback circuits to guarantees the efficient feedback correction of control system as the output feedback channel is disconnected. Finally, the dynamic feedback structure composed by measured state variables of control system that can be able to inhibit the unpredictable interference in advance.

The organization of this paper is as follows: In Section 2, the proposed integration between state feedback predictive control strategy and the T-S fuzzy model is introduced. In Section 3, a non-linear model of the hydro-turbine governing system is defined. The application of the approach to a realistic case-study and the numerical experiment results obtained are then proposed in Section 4 and Section 5, respectively. Conclusions and discussion in Section 6 close the paper.

## 2. Proposed strategy

### 2.1 T-S fuzzy model

A non-linear system can be described as:

$$\begin{cases} \dot{\boldsymbol{x}}(t) = \boldsymbol{f}(\boldsymbol{x}(t), \boldsymbol{u}(t)) \\ \boldsymbol{y} = \boldsymbol{C}\boldsymbol{x}(t) \end{cases}, \tag{1}$$

where $\boldsymbol{x}(t) \in \boldsymbol{R}^n$ and $\boldsymbol{u}(t) \in \boldsymbol{R}^n$ satisfy the conditions $\boldsymbol{x}(t) \in X$, $\boldsymbol{u}(t) \in U$ with $\forall t \geq 0$, $\boldsymbol{f}(\cdot)$ is a Lipschitz continuous function in the space $X \times U$, and $\boldsymbol{y}$ is the output response of the nonlinear system.

In order to approximate the non-linear system, the T-S fuzzy model has been adopted, according to the study by (Wang et al. 2006), the discrete T-S fuzzy state space model can be expressed as:

$R_p^i$: If $x_1(k)$ is $M_1^i$, and $x_2(k)$ is $M_2^i$, .....and $x_n(k)$ is $M_n^i$, then

$$\boldsymbol{x}(k+1) = \boldsymbol{A}_i \boldsymbol{x}(k) + \boldsymbol{B}_i \boldsymbol{u}(k) + \boldsymbol{W}_i, \tag{2}$$

where $i=1,2,\cdots,l$; $R_p^i$ denotes the $i-th$ fuzzy rules of the T-S fuzzy model; $l$ is the number of rules; $M_j^i$ ( $j=1,2,\cdots,n$ ) denotes fuzzy collection; $\boldsymbol{x}(k)=[x_1(k), x_2(k),\cdots,x_n(k)]^T \in \boldsymbol{R}^n$ is the state variable; $\boldsymbol{A}_i \in \boldsymbol{R}^{n\times n}$ and $\boldsymbol{B}_i \in \boldsymbol{R}^{n\times m}$ denote respectively the system matrix and control matrix of the $i-th$ subsystem; $\boldsymbol{u}(k) \in \boldsymbol{R}^n$ is the input variable; $\boldsymbol{W}_i$ is the constant vector of the $i-th$ subsystem, which is generally considered to be a zero vector, according to the fuzzy modeling method.

Hence, if $\boldsymbol{y}(k)=[\boldsymbol{y}_1(k) \quad \boldsymbol{y}_2(k),\cdots,\boldsymbol{y}_m(k)]^T$ , and $\boldsymbol{C}=[\boldsymbol{c}_1^T,\boldsymbol{c}_2^T,\cdots,\boldsymbol{c}_m^T]^T \in \boldsymbol{R}^{m\times n}$ denote the system output matrix, the Eq. (3) is obtained:

$$\boldsymbol{y}(k)=\boldsymbol{C}\boldsymbol{x}(k). \tag{3}$$

**2.2 Feedback predictive control based on the T-S fuzzy model**

The block diagram of the state feedback predictive control under study in this work is shown in **Fig. 1**. With regard to the diagram, $\hat{y}$ denotes the prediction output obtained by the model inference, $y$ denotes the actual output of the controlled process, and $x$ is a state variable. In the proposed strategy, the state feedback predictive control is performed on the basis of the T-S fuzzy model. The output for the state feedback predictive control is obtained according to the procedure described in the following.

**Figure 1.** Block diagram of the state feedback predictive control based on the T-S fuzzy model

On the basis of the fuzzy modeling approach, if the vector $\boldsymbol{W}_i$ in Eq. (2) is considered to be a zero vector, then the same equation can be expressed as:

$$x(k+1)=\sum_{i=1}^{l}h_i(k)\boldsymbol{A}_i x(k)+\sum_{i=1}^{l}h_i(k)\boldsymbol{B}_i(k)u(k)\,. \tag{4}$$

For the sake of clarity, we set $\boldsymbol{H}_{jA}=\sum_{i=1}^{l}h_i(k+1)\boldsymbol{A}_i, \boldsymbol{H}_{jB}=\sum_{i=1}^{l}h_i(k+1)\boldsymbol{B}_i,$ then

$$\begin{aligned} x(k+p)=&\boldsymbol{H}_{(p-1)A}\boldsymbol{H}_{(p-2)A}\cdots\boldsymbol{H}_{0A}x(k)\cdots\\ &+\boldsymbol{H}_{(p-1)A}\boldsymbol{H}_{(p-2)A}\cdots\boldsymbol{H}_{1A}\boldsymbol{H}_{0B}u(k)\cdots\\ &+\boldsymbol{H}_{(p-1)A}\boldsymbol{H}_{(p-2)B}u(k+p-2)+\boldsymbol{H}_{(p-1)B}u(k+p-1) \end{aligned}\,. \tag{5}$$

$\boldsymbol{H}_{jA}$ and $\boldsymbol{H}_{jB}$ are associated to $x(k+q)$ through the derivation process described above. In this case, the membership function under for state $x^s$ results $h_i^s=\dfrac{\mu^i(x^s)}{\sum_{j=1}^{l}\mu^j(x^s)}$, where $i=1,2,\cdots,l$.

Considering $h_i(k+q)=h_i^s$, $q=1,2\cdots p$, then the former conditions become:

$$\begin{aligned} &\boldsymbol{H}_{(p-1)A}=\boldsymbol{H}_{(p-2)A}=\cdots=\boldsymbol{H}_{1A}=\sum_{i=1}^{l}h_j^s\boldsymbol{A}_i\xrightarrow{define}\boldsymbol{A}\\ &\boldsymbol{H}_{(p-1)B}=\boldsymbol{H}_{(p-2)B}=\cdots=\boldsymbol{H}_{1B}=\sum_{i=1}^{l}h_j^s\boldsymbol{B}_i\xrightarrow{define}\boldsymbol{B} \end{aligned}\,. \tag{6}$$

In light of Eq. (6), Eq. (5) can be rewritten in the form:

$$x(k+p)=\boldsymbol{A}^p x(k)+\sum_{i=1}^{p}\boldsymbol{A}^{(i-1)}\boldsymbol{B}u(k+p-i)\,. \tag{7}$$

Eq. (7) suggests that to each sample of $p_j$, the estimated value of the $j-th$ output can be defined as:

$$\hat{y}_j(k+p_j)=C_j\boldsymbol{A}^{p_j}x(k)+\sum_{i=1}^{p_j}C_j\boldsymbol{A}^{i-1}\boldsymbol{B}u(k+p_j-i)\,, \tag{8}$$

where $j=1,2\cdots m$, and $p_j$ is the prediction horizon of the $j-th$ output component $y_j(k)$.

For single-valued state feedback predictive control algorithms, the control horizon is L=1. This implies that the control law is subject to modifications only at the time k, while it maintains a constant value in the rest of the time domain (namely $u(k+i)=u(k), i>0$).

In light of this, Eq. (8) can be expressed as

$$\hat{y}_j(k+p_j)=C_j\boldsymbol{A}^{p_j}x(k)+\boldsymbol{S}_j(p_j)u(k), \tag{9}$$

where $\boldsymbol{S}_j(p_j)=\sum_{i=1}^{p_j}C_j\boldsymbol{A}^{i-1}\boldsymbol{B}, j=1,2,\cdots,m$.

On the other hand, the feedback compensation of the estimated output results:

$$Y_{cj}(k+p_j)=\hat{y}_j(k+p_j)+y_j(k)-\hat{y}_j(k), \tag{10}$$

where $\hat{y}_j(k)=C_j\boldsymbol{A}^{p_j}x(k-p_j)+\sum_{i=1}^{p_j}C_j\boldsymbol{A}^{i-1}\boldsymbol{B}u(k-i)$, it is the prediction value of the component $y_j(k)$, using the history state $x(k)$ and the history control $u(k)$.

**2.3 Optimal control**

$Y_j^s(k+p_j)$ is set-point of the $j-th$ output. Then the predictive error of the $j-th$ output is:

$$e_j=Y_j^s(k+p_j)-y_{cj}(k+p_j). \tag{11}$$

Introducing Eq. (9) in Eq. (11) it results:

$$e_j=Y_j^s(k+p_j)-\hat{y}_j(k+p_j)-y_j(k)+\hat{y}_j(k), \tag{12}$$

which becomes:

$$e_j=Y_j^s(k+p_j)-C_jA^{p_j}x(k)-S_j(p_j)u(k)-y_j(k)+\hat{y}_j(k). \tag{13}$$

Under the assumption $E=\left[e_1,e_2,\cdots,e_m\right]^T$, Eq. (13) can be rewritten as:

$$E=Y^s(k)-\boldsymbol{K}x(k)-\boldsymbol{S}(p)u(k)-y(k)+\hat{y}(k), \tag{14}$$

where $y(k)=[y_1(k),y_2(k),\cdots,y_m(k)]^T$, $\hat{y}(k)=[\hat{y}_1(k),\hat{y}_2(k),\cdots,\hat{y}_m(k)]^T$,

$$Y^s(k)=\begin{pmatrix} Y_1^s(k+p_1) \\ Y_2^s(k+p_2) \\ \vdots \\ Y_m^s(k+p_m) \end{pmatrix},\ \boldsymbol{K}=\begin{pmatrix} C_1A^{p_1} \\ C_2A^{p_2} \\ \vdots \\ C_mA^{p_m} \end{pmatrix} \text{ and } \boldsymbol{S}(p)=\begin{pmatrix} S_1(p_1) \\ S_2(p_2) \\ \vdots \\ S_m(p_m) \end{pmatrix}. \quad (15)$$

The objective function of the problem under study is then expressed as:

$$J=E^T\boldsymbol{Q}E, \quad (16)$$

where Q is a positive definite symmetric matrix. Imposing $\frac{\partial J}{\partial u}=0$, the optimal control law of the $i-th$ subsystem results:

$$u(k)=\boldsymbol{S}^{-1}(p)[Y^s(k)-\boldsymbol{K}x(k)-y(k)+\hat{y}(k)]. \quad (17)$$

Eq. (17) shows that the optimal control law of the system is composed of the state feedback control law and the output feedback control law.

The procedure of the described algorithm is summed up by the flowchart show in **Fig 2**:

**Figure 2.** Flowchart of state feedback predictive control

### 2.4 Stability analysis

Assuming the model to be accurate and without any disturbance, the condition $y(k)=\hat{y}(k)$ is verified.

Eq. (17) can be expressed as:

$$u(k)=\boldsymbol{S}^{-1}(p)[Y^s(k)-\boldsymbol{K}x(k)]. \quad (18)$$

Moreover, the state space of the closed-cycle predictive control system can be expressed as:

$$\begin{cases} x(k+1) = \boldsymbol{A}_c x(k) + \boldsymbol{B}_c Y^s(k) \\ y(k) = \boldsymbol{C}x(k) \end{cases}, \tag{19}$$

where $\boldsymbol{A}_c = \boldsymbol{A} - \boldsymbol{B}\boldsymbol{S}^{-1}(p)\boldsymbol{K}$, $\boldsymbol{B}_c = \boldsymbol{B}\boldsymbol{S}^{-1}(p)$.

Then Eq. (2) (always assuming $\boldsymbol{W} = \boldsymbol{0}$) becomes:

$$x(k+1) = \sum_{i=1}^{l} h_i(k)(\boldsymbol{A}_i - \boldsymbol{B}_i\boldsymbol{S}^{-1}(p)\boldsymbol{K})x(k) + \sum_{i=1}^{l} h_i\boldsymbol{B}_i\boldsymbol{S}^{-1}(p)Y^s(k). \tag{20}$$

Since the stability of the closed -cycle system is not related to the value of $Y^s(k)$. we assume $Y_s(k) = [0,0,0]^T$. In this case, Eq. (20) can be simplified as:

$$x(k+1) = \sum_{i=1}^{l} h_i(k)(\boldsymbol{A}_i - \boldsymbol{B}_i\boldsymbol{S}^{-1}(p)\boldsymbol{K})x(k). \tag{21}$$

**Theorem:** If there exists a positive definite symmetric matrix $\boldsymbol{P}_i$ satisfying the linear matrix inequality:

$$\begin{bmatrix} \boldsymbol{P}_i & \boldsymbol{G}_i^T\boldsymbol{P}_r \\ \boldsymbol{P}_r\boldsymbol{G}_i & \boldsymbol{P}_r \end{bmatrix} > 0, \boldsymbol{G}_i = \boldsymbol{A}_i - \boldsymbol{B}_i\boldsymbol{S}^{-1}(p)\boldsymbol{K}, i, r = 1,2,\cdots,l. \tag{22}$$

Then the T-S fuzzy closed-cycle system is global asymptotic stability under the control law of Eq. (17).

**Proof:** The Lyapunov function for the system described by Eq. (21) is:

$$V(x(k)) = x(k)^T\boldsymbol{P}(x(k))x(k), \boldsymbol{P}(x(k)) = \sum_{r=1}^{l} h_r(k)\boldsymbol{P}_r. \tag{23}$$

Then $\Delta V = V(x(k+1)) - V(x(k))$

$$= x(k+1)^T\sum_{r=1}^{l} h_r(k+1)\boldsymbol{P}_r x(k+1) - x(k)^T\boldsymbol{P}(x(k))x(k), \tag{24}$$

where $h_r(k)$ is the weight of the fuzzy rule, and verifies the conditions of $0 \le h_i(k) \le 1$ and $\sum_{i=1}^{l} h_i(k) = 1$. In light of this,

$$\Delta V = [\sum_{i=1}^{l} h_i(k)\boldsymbol{G}_i x(k)]^T \sum_{i=1}^{l} h_r(k+1)\boldsymbol{P}_r[\sum_{j=1}^{l} h_j(k)\boldsymbol{G}_j x(k)] - x(k)^T[\sum_{i=1}^{l} h_i(k)\boldsymbol{P}_i]x(k)$$
$$= \sum_{i=1}^{l}\sum_{j=1}^{l}\sum_{r=1}^{l} h_i(k)h_r(k+1)h_j(k)x(k)^T[\boldsymbol{G}_i^T\boldsymbol{P}_r\boldsymbol{G}_j - \boldsymbol{P}_i]x(k) \quad (25)$$

Being $\boldsymbol{P}_r$ is a positive definite symmetric matrix, it can be written as: $\boldsymbol{P}_r = \boldsymbol{D}_r\boldsymbol{D}_r$. Hence Eq. (25) becomes:

$$\Delta V = \sum_{i=1}^{l}\sum_{j=1}^{l}\sum_{r=1}^{l} h_i(k)h_r(k+1)h_j(k)x(k)^T[\boldsymbol{G}_i^T\boldsymbol{P}_r\boldsymbol{G}_j - \boldsymbol{P}_i]x(k)$$
$$\le \sum_{i=1}^{l}\sum_{j=1}^{l}\sum_{r=1}^{l} h_i(k)h_r(k+1)h_j(k)x(k)^T[\frac{1}{2}(\boldsymbol{G}_i^T\boldsymbol{D}_r\boldsymbol{D}_r\boldsymbol{G}_i + \boldsymbol{G}_j^T\boldsymbol{D}_r\boldsymbol{D}_r\boldsymbol{G}_j) - \boldsymbol{P}_i]x(k) \quad (26)$$
$$== \sum_{i=1}^{l}\sum_{r=1}^{l} h_i(k)h_r(k+1)x(k)^T[\boldsymbol{G}_i^T\boldsymbol{P}_r\boldsymbol{G}_i - \boldsymbol{P}_i]x(k)$$

According to the Schur complement of the matrix, the inequality in Eq. (22) holds only under the condition $\boldsymbol{P}_i - \boldsymbol{G}_i^T\boldsymbol{P}_r\boldsymbol{G}_i > 0$, it is equivalent to $\boldsymbol{G}_i^T\boldsymbol{P}_r\boldsymbol{G}_i - \boldsymbol{P}_i < 0$, besides, $h_i(k) \ge 0, h_r(k+1) \ge 0$, then:

$$\Delta V \le \sum_{i=1}^{l}\sum_{r=1}^{l} h_i(k)h_r(k+1)x(k)^T\left[\boldsymbol{G}_i^T\boldsymbol{P}_r\boldsymbol{G}_i - P_i\right]x(k) < 0. \quad (27)$$

The closed-loop system Eq. (21) is globally asymptotical stability.

## 3. Non-linear modeling of the HTGS

The HTGS modeled in this paper consists of a hydro-turbine system, a penstock system, a generator system, and a servo system. The structure of such system is shown in the diagram of **Fig 3**.

**Figure 3.** Structure diagram of the hydro-turbine and penstock system

### 3.1 Hydro-turbine and pressure diversion system

From Ref (Zhang et al., 2015), the transfer function of the pressure in the

diversion system can be expressed as:

$$G_h(s) = -2h_w \frac{\frac{1}{48}T_r^3 s^3 + \frac{1}{2}T_r s}{\frac{1}{8}T_r^3 s^2 + 1}, \tag{28}$$

where $h_w$ is the characteristic parameter of the penstock system, $T_r = \frac{2L}{v}$ is the time constant of the elastic water hammer.

When the hydraulic turbine is not subject to significant load changes, the speed relative deviation can be regarded as $\omega = 0$, the relationship between the hydraulic turbine torque $m_t$ and the output power $P_m$ is obtained as:

$$P_m = m_t . \tag{29}$$

Therefore, the transfer function for the hydro-turbine and the diversion system can be written as:

$$G_t(s) = e_y \frac{1 + eG_h(s)}{1 - e_{qh}G_h(s)}, \tag{30}$$

where $e_y$, $e$, $e_{qh}$ denote the main servomotor stroke transfer coefficient, the intermediate variable and the head transfer coefficient of the flow rate, respectively.

Based on Eq. (28) and Eq. (30), the Eq. (30) can be expressed as:

$$G_t(s) = -\frac{e_y}{e_{qh}} \frac{es^3 - \frac{3}{h_w T_r}s^2 + \frac{24e}{T_r^2}s - \frac{24}{h_w T_r^3}}{s^3 + \frac{3}{e_{qh}h_w T_r}s^2 + \frac{24}{T_r^2}s + \frac{24}{e_{qh}h_w T_r^3}}, \tag{31}$$

According to Eq. (30), the state space equations of the hydro-turbine and penstock system can be rewritten as:

$$\begin{cases} \dot{x}_1 = x_2 \\ \dot{x}_2 = x_3 \\ \dot{x}_3 = -a_0 x_1 - a_1 x_2 - a_2 x_3 + y \end{cases}. \tag{32}$$

The dynamic equation of the hydro-turbine output torque can be results:

$$m_t = b_3 y + (b_0 - a_0 b_3) x_1 + (b_1 - a_1 b_3) x_2 + (b_2 - a_2 b_3) x_3 , \tag{33}$$

where $x_1$, $x_2$ and $x_3$ are state variables, $a_0 = \frac{24}{e_{qh} h_w T_r^3}$, $a_1 = \frac{24}{T_r^2}$, $a_2 = \frac{3}{e_{qh} h_w T_r}$, $b_0 = \frac{24 e_y}{e_{qh} h_w T_r^3}$, $b_1 = - \frac{24 e e_y}{e_{qh} T_r^2}$, $b_2 = \frac{3 e_y}{e_{qh} h_w T_r}$ and $b_3 = - \frac{e e_y}{e_{qh}}$.

### 3.2 Generator system

The generator system has been modeled adopting a second-order non-linear model, for which the state equation is expressed as:

$$\begin{cases} \dot{\delta} = \omega_0 \omega \\ \dot{\omega} = \frac{1}{T_{ab}} \left[ m_t - m_e - D\omega \right] \end{cases}, \tag{34}$$

where $\delta$, $\omega$, $T_{ab}$ and $D$ denote respectively the rotor angle, the deviation of the generator rotor speed, the unit mechanical inertia time constant and the damping coefficient.

If the influence of the rotor speed variation on the torque is expressed in terms of its impact on the damping coefficient, the electromagnetic torque of the generator ($m_e$) results equal to the electromagnetic power ($P_e$), as shown in Eq. (35).

$$m_e = P_e . \tag{35}$$

Furthermore, the electromagnetic power of the salient rotor hydro-generator can be expressed as:

$$P_e = \frac{E'_q V_s}{x'_{d\Sigma}} \sin\delta + \frac{V_s^2}{2} \frac{x'_{d\Sigma} - x'_{q\Sigma}}{x'_{d\Sigma} x'_{q\Sigma}} \sin 2\delta , \tag{36}$$

where $E'_q$ is the transient voltage of the $q$ axis, $V_s$ is the infinite bus voltage, $x'_d$ is the direct axis transient reactance and $x'_q$ is the quartered axis reactance, $x'_{d\Sigma}$

and $x'_{q\Sigma}$ can be expressed as:

$$\begin{cases} x'_{d\Sigma} = x'_d + x_T + \frac{1}{2}x_L \\ x'_{q\Sigma} = x'_q + x_T + \frac{1}{2}x_L \end{cases}, \tag{37}$$

where $x_T$ is the short-circuit reactance of the transformer, and $x_L$ is the transmission line reactance.

### 3.3 Hydraulic automatic system

The dynamic characteristics of a hydraulic automatic system are represented in Eq. (38):

$$T_y \frac{dy}{dt} + y = u_y, \tag{38}$$

where $y$, $T_y$ and $u_y$ denote the incremental deviation of the main servomotor stroke, the response time constant of the servomotor and the control signal, respectively.

From Eq. (28) to Eq. (38), the six-dimension mathematical model of the HTGS firstly proposed in Section 3 can be described as:

$$\begin{cases} \dot{x}_1 = x_2 \\ \dot{x}_2 = x_3 \\ \dot{x}_3 = -a_0 x_1 - a_1 x_2 - a_2 x_3 + y \\ \dot{\delta} = \omega_0 \omega + u_1 \\ \dot{\omega} = \frac{1}{T_{ab}}\left[ m_t - \frac{E'_q V_s}{x'_{d\Sigma}} \sin\delta - \frac{V_s^2}{2} \frac{x'_{d\Sigma} - x'_{q\Sigma}}{x'_{d\Sigma} x'_{q\Sigma}} \sin 2\delta - D\omega \right] + u_2 \\ \dot{y} = \frac{1}{T_y}(u_3 - y) \end{cases}, \tag{39}$$

where $u_1$, $u_2$ and $u_3$ are respectively the three predictive controllers considered. In order to perform a realistic numerical analysis of the model, system parameters were selected for the input of the model: $\omega_0$=314 rad/s, $T_{ab}$=8.0, $D$=0.5, $E'_q$=1.35,

$x'_{d\Sigma}$=1.15, $x'_{q\Sigma}$=1.474, $T_y$=0.1, $V_s$=1.0, $e_{qh}$=0.5, $e_y$=1.0, $e$=0.7, $T_r$=1.0, $h_w$=2.0, $r$=0, $a_0$=24, $a_2$=3, $b_0$=24, $b_1$ = -33.6, $b_2$=3, $a_1=\frac{24}{T_r^2}$, and $b_3$ = -1.4, respectively.

## 4. Optimal predictive controller design

The T-S fuzzy model is adopted in the present section to linearize the hydro-turbine governing system model previously implemented. The procedure followed consists of various steps as shown in the following:

Rule $i$: IF $\delta(t)$ is $F_i$, then $\begin{cases}\dot{\boldsymbol{x}}(t)=\boldsymbol{A}_i\boldsymbol{x}(t)+\boldsymbol{B}_i\boldsymbol{u}(t)\\ \dot{\boldsymbol{y}}(t)=\boldsymbol{C}_i\boldsymbol{x}(t)\end{cases}$, $i$=1,2,3,4

where $F_1=\frac{1}{4}\left(1+\frac{\delta^2}{v^2}\right)$, $F_2=\frac{1}{4}\left(1-\frac{\delta^2}{v^2}\right)$, $F_3=\frac{1}{4}\left(1+\frac{\delta^4}{v^4}\right)$, $F_4=\frac{1}{4}\left(1-\frac{\delta^4}{v^4}\right)$, v=1.6.

In the current study, a discretization step of 0.02s was adopted in order to obtain an acceptable representation of the initial data.

Based on the above analysis, the four subsystems by the linearization procedures are discretized as:

$$x(k+1)=\boldsymbol{M}_i x(k)+\boldsymbol{N}_i u(k), i=1,2,3,4. \tag{40}$$

On the basis of the optimal control law deduced from the former analysis and Eq. (15), the feedback gain $\boldsymbol{K}_i$ and inverse matrix $\boldsymbol{S}_i^{-1}$ are easily obtained as:

**Subsystems 1：**

$$K_1=\begin{bmatrix}34.2022 & -4.6939 & 4.0229 & 0.5393 & 52.4755 & -0.3704\\ 0.8954 & -0.1982 & 0.0969 & -0.0134 & 0.5293 & -0.0047\\ 0 & 0 & 0 & 0 & 0 & 0.1353\end{bmatrix},$$

$$\boldsymbol{S}_1^{-1}=\begin{bmatrix}4.5767 & -157.4012 & -0.3589\\ 0.0364 & 4.7181 & 0.0777\\ 0 & 0 & 1.1564\end{bmatrix}.$$

**Subsystem 2：**

$$K_2=\begin{bmatrix}33.9612 & -4.6746 & 3.9971 & 0.5420 & 51.9193 & -0.3675\\ 0.8850 & -0.1970 & 0.0958 & -0.0133 & 0.5147 & -0.0046\\ 0 & 0 & 0 & 0 & 0 & 0.1353\end{bmatrix},$$

$$\boldsymbol{S}_2^{-1}=\begin{bmatrix}4.5756 & -158.0435 & -0.3598\\ 0.0367 & 4.7902 & 0.0782\\ 0 & 0 & 1.1564\end{bmatrix}.$$

**Subsystem 3：**

$$K_3=\begin{bmatrix}34.2309 & -4.6908 & 4.0233 & 0.5393 & 52.5323 & -0.3705\\ 0.8988 & -0.1985 & 0.0972 & -0.0134 & 0.5334 & -0.0047\\ 0 & 0 & 0 & 0 & 0 & 0.1353\end{bmatrix},$$

$$\boldsymbol{S}_3^{-1}=\begin{bmatrix}4.5769 & -157.1056 & -0.3596\\ 0.0366 & 4.7311 & 0.0781\\ 0 & 0 & 1.1564\end{bmatrix}.$$

**Subsystem 4：**

$$K_4=\begin{bmatrix}34.2798 & -4.6974 & 4.0291 & 0.5387 & 52.6087 & -0.3711\\ 0.8985 & -0.1985 & 0.0972 & -0.0134 & 0.5328 & -0.0047\\ 0 & 0 & 0 & 0 & 0 & 0.1353\end{bmatrix},$$

$$\boldsymbol{S}_4^{-1}=\begin{bmatrix}4.5768 & -157.2653 & 0.1439\\ 0.0364 & 4.7068 & 0.1730\\ 0 & 0 & 11.5837\end{bmatrix}.$$

## 5. Numerical results

To illustrate the performance of the novel method proposed, the parameters for the numerical application were selected form realistic range: the prediction horizon is equal to 10 ($P$=10), the control horizon to 1 ($L$=1), the softness factor to 0.15 ($e$= 0.15), the sampling period as mentioned is 0.02s, and the initial values are set as

$[x_1, x_2, x_3, d, \omega, y]^T = [0.01, 0.01, 0.01, 0.01, 0.01, 0.01]^T$ .

**Case 1: Model match**

The output responses for the variables $\delta, \omega, y$ of the non-linear hydro-turbine governing model with the references $Y_s = [1.5, 0.1, 0.8]^T$ are shown in **Fig 4**.

**Figure 4.** Output responses for the variables $d, \omega, y$ of the system with T-S SFPC controllers; (a) $\delta$ (b) $\omega$ (c) $y$

The results obtained highlight that the output response of the variables $\delta$ and $\omega$ approach the reference $Y_s$ quite rapidly, matching it for at only t=3.5s; furthermore, the fluctuation frequency and overshoot result relatively small. These trends indicate that when the load is affected by periodic fluctuations, the controller can guarantee that the effective and fast accomplishment of the equilibrium between the active torque and the resistance torque of the hydroelectric unit. In addition to this, the frequency of the fluctuations the unit can be maintained within acceptable values.

As shown in **Fig. 4 (c)**, the stability of the main servomotor stroke $y$ can be controlled optimally, accomplishing response times within one second and without overshoot. Due to the approximate linear relationship between the main servomotor stroke $y$ and guide vane opening $\alpha$, which implies the controller to regulate the guide vane so that the hydraulic turbine flow is maintained constant. To sum up, these first results proof the reliability of predictive controllers which are able to lead the system to stability in short time.

**Case 2: Tracking performance**

Let now assume the variables $\delta, \omega, y$ to continuously adjust to the variation of working conditions. In this case the values of reference for the output are selected as: $Y_s = [1.5, 0.1, 0.8]^T$, $0 \le t \le 8s$ ; $Y_s = [1.7, 0.12, 1.0]^T$, $8s \le t \le 14s$ ; $Y_s = [1.7, 0.12, 1.0]^T$, $14s \le t \le 20s$ . The results of the analysis performed are shown in **Fig. 5**.

**Figure 5.** Servo tracking response curves under different set points; (a) $\delta$ (b) $\omega$ (c) $y$

**Fig. 5** suggests that the servo tracking speed of the system as well as the output response curves are stationary. This indicates that the system is characterized by an excellent tracking performance adopting the novel control method. More specifically, the output can track the load variation in real-time, so that the hydroelectric generating unit adjusts output power in time and keeps the unit frequency fluctuating within the specified range.

**Case 3: Disturbance analysis**

During the daily operation of hydropower stations, the system is subject to a wide range of perturbation, possibly caused by the variation or even rejection of the load as well as shutdown procedures etc. Thus, to study the realistic performance of the state feedback predictive control system under these conditions, the HTGS model was applied assuming the occurrence of disturbances for the state variables $\delta, \omega$ and $y$, so that: $d_1 = [0.1, 0.03, 0.1]^T$, $10s \le t \le 12s$ . Then, the estimated response of the

hydroelectric system is shown in **Fig. 6**.

**Figure 6.** System response in the case of perturbations affecting $\delta, \omega, y$ ; (a) $\delta, 10s \le t \le 12s, d = 0.1$ (b) $\omega, 10s \le t \le 12s, d = 0.03$ (c) $y, 10s \le t \le 12s, d = 0.1$

In spite of the perturbations assumed, also in this case the system appears able to achieve stability. Most importantly, the fluctuation range and the overshoot relatively small, it proving that the HTGS can enter the stable state quickly under the control of the state feedback controller, even if it subject to frequency and load disturbance. Hence, the analysis suggests that the proposed method ensures a good degree of immunity of the controller to interferences.

**Case 4: Model mismatch**

Former studies available in the literature suggest that steady surges, non-linear processes and external disturbances of the system can lead to model mismatch in long-running predictive control system operation. Therefore, to test the control performance of the state feedback predictive algorithm against these cases, the occurrence of errors affecting the model parameters, $\Delta A \neq 0$, $\Delta B \neq 0$ and $\Delta C \neq 0$ have been considered with regard to the predictive model. The control performance estimated considering such initial imprecision in the parameters is shown in **Fig. 7**.

**Figure 7.** Response curves for the variables $\delta, \omega, y$ assuming different error values of the input parameters

**Fig. 7** show that the proposed method enables the HTGS reach to stability rapidly, with only small fluctuations and overshoot. Therefore, it shows that the state feedback predictive control system based on T-S fuzzy model can have a good control performance in overcome model mismatch problems, and provide a strong robustness.

**Case 5: Effects of the prediction horizon**

A further phase of the current study focused on the analysis of the impact of the prediction horizon on the performance of the approach. In this part, prediction horizon $P$ is regarded as a variable parameter, the control effects of the $P$ are presented in **Fig. 8**.

**Figure 8.** Response curves $d, \omega, y$ for assuming different prediction horizon values; (a) $\delta$ (b) $\omega$ (c) $y$

As shown by the response curve in **Fig. 8**, long prediction horizon values result in larger overshoot of the system. Therefore, to select a suitable value of the operational prediction horizon, one of the first things to consider is that a positive definite symmetric matrix $\boldsymbol{P}_i$ can be found which satisfy the linear matrix inequalities (22), this condition ensures the closed-cycle system is global asymptotic stability under the control law (17). In addition, the estimated response rate, overshoot and fluctuation range are comprehensively considered. Consequently, the prediction horizon is equal to 10 ( $P = 10$ ) adopted in this paper.

**Case 6: Comparison including the MPC, the PID and the T-S SFPC approach**

In order to validate the T-S SFPC method proposed in the paper compared with MPC (Diehl et al., 2002 and 2005; Kunisaki et al., 2008; Kirches et al., 2012; Lopez-Negrete et al., 2013; Jaschke et al., 2014; Otsuka et al., 2017; La et al., 2017) and the PID (Ntogramatzidis et al., 2011) methods, a comparative analysis is therefore performed. Here, the PID controller by Ntogramatzidis in the system (39) is expressed as:

$$\begin{cases} \dot{x}_1 = x_2 \\ \dot{x}_2 = x_3 \\ \dot{x}_3 = -a_0 x_1 - a_1 x_2 - a_2 x_3 + y \\ \dot{\delta} = \omega_0 \omega \\ \dot{\omega} = \dfrac{1}{T_{ab}}\left[ m_t - \dfrac{E'_q V_s}{x'_{d\Sigma}} \sin\delta - \dfrac{V_s^2}{2} \dfrac{x'_{d\Sigma} - x'_{q\Sigma}}{x'_{d\Sigma} x'_{q\Sigma}} \sin 2\delta - D\omega \right] \\ \dot{y} = \dfrac{1}{T_y}\left(-k_p(r-\omega) - \dfrac{k_i}{\omega_0}\delta - k_d D^q \omega - y\right) \end{cases}, \tag{41}$$

where $k_p, k_i$ and $k_d$ are PID parameters. The parameters are $k_p = 2.0$, $k_i = 1.0$ and $k_d = 2.0$, $q = 1$.

The initial assumption for the reference solution is $Y_s = [0,0,0]^T$. Then, numerical results of MPC, PID and T-S SFPC are shown in **Fig. 9.**

**Figure 9.** Comparison of control performance obtained with MPC, PID and T-S SFPC approaches; (a) $\delta$ (b) $\omega$ (c) $y$

**Table 1** Adjusting time of the HTGS under MPC, PID and T-S SFPC controllers

The performance results associated with the PID, MPC and T-S SFPC are shown in **Fig. 9** and **Table 1**. It is obvious that the state feedback predictive controller proposed in this paper allows providing better performance for non-linear hydropower system than both PID and MPC. As highlighted in Table 1, compared with MPC, the T-S SFPC can enable the adjusting time of both outputs $\delta$ and $\omega$ to shorten by 25% and 22.4%. Furthermore, the fluctuations of the state feedback predictive control method are smaller than those registered for PID and MPC controllers. This implies

that the T-S SFPC method is more efficient than the traditional PID approach and MPC in monitoring and acting on the state of the hydropower station on a real-time scale. Thus, the T-S SFPC enjoys an excellent performance in control of the nonlinear hydropower system.

## 6. Conclusions and discussions

In this paper, the state feedback predictive control algorithm based on the T-S fuzzy model is proposed for hydro-turbine governing systems. It is based on the application of the T-S fuzzy approach to a nonlinear six-dimensional hydroelectric plant system. The proposed methodology not only improves the precision of the prediction model, but also represents accurately the dynamic characteristics of the hydroelectric system. In addition to this, the global asymptotic stability theorem of the close-loop system is proved through the use of the discrete Lyapunov function and Schur complements of matrices. In order to verify the effectiveness and the efficiency of the proposed method, this is applied to a nonlinear hydropower plant system. The results obtained from the numerical analysis, the highlight excellent control performance of the proposed control method in the case of external disturbances, Servo tracking and model mismatch. In the final stage, the novel proposed control method was compared with traditional PID and MPC methods, demonstrating the unquestionable advantages of the proposed method in the non-linear system. And it is worth noting that the results obtained by the overall analysis performed of the T-S SFPC method can provide strong robustness, perfect tracking performance and great anti-interference performance. In conclusion, the T-S SFPC method is a capable control tool particularly suitable for complex non-linear hydroelectric plant systems.

Future research work will focus on how to solve the problem of predictive control optimization for high-dimensional systems with input constraints and state delays via intelligent optimization algorithms.

**Acknowledgements**

This work was supported by the scientific research foundation of Natural Science Foundation (51479173, 51279167), Fundamental Research Funds for the Central Universities (201304030577), Scientific research funds of Northwest A&F University (2013BSJJ095), the scientific research foundation on water engineering of Shaanxi Province (2013slkj-12), the Science Fund for Excellent Young Scholars from Northwest A&F University and Shaanxi Nova program (2016KJXX-55).

**References**

Brown R, Pusey J, Murugan M and Le D (2013) Generalized predictive control algorithm of a simplified ground vehicle suspension system. *Journal of Vibration Control* doi: 10.1177/1077546312448505.

Chen ZH, Yuan YB, Yuan XH, Huang YH, Li XS and Li WW (2015) Application of multi-objective controllers to optimal tuning of PID gains for a hydraulic turbine regulating system using adaptive grid particle swam optimization. *Isa Transactions* 56: 173-187.

Cortes P, Kazmierkowski MP, Kennel RM, Quevedo DE and Rodriguez J (2008) Predictive control in power electronics and drives. *IEEE Transactions on Industrial Electronics* 56: 4312-4324.

Chen DY, Zhao WL, Sprott JC and Ma XY (2013) Application of Takagi-Sugeno fuzzy model to a class of chaotic synchronization and anti-synchronization. *Nonlinear Dynamics* 73: 1495-1505.

Donaisky E, Oliveira GHC, Santos EAP, Leandro GV, Pena AM and Souza JA (2015) Hybrid model predictive control as a LFC solution in hydropower plants. *4th International Conference on Mechanics and Control Engineering (ICMCE)*, Lisbon, Portugai, 35.

Dutta A, Lonescu C, Loccufier M and De Keyser R (2016) Robust penalty adaptive model predictive control of constrained, underdamped, noncollocated systems. *Journal of Vibration Control* doi: 10.1177/1077546314534282.

Diehl M, Findeisen R, Allgower F, Bock HG and Schloder JP (2005) Nominal stability of real-time iteration scheme for nonlinear model predictive control. *IEE Proceedings-Control Theory and Applications* 152:296-308.

Diehl M, Bock HG, Schloder JP, Findeisen R, Nagy Z and Allgower F (2002) Real-time optimization and nonlinear model predictive control of processes governed by differential-algebraic equations. *Journal of Process Control* 12:577-585.

Errouissi R, Yang J, Chen WH and Al-Durra A (2016) Robust nonlinear generalized predictive control for a class of uncertain nonlinear systems via an integral sliding mode approach. *International Journal of Control* 89: 1698-1710.

Guo WC, Yang JD, Wang MJ and Lai X (2015) Nonlinear modeling and stability analysis of hydro-turbine governing system with sloping ceiling tailrace tunnel under load disturbance. *Entergy Conversion and Management* 106: 127-138.

Hao Y (2000) Theory and application of a novel fuzzy PID controller using a simplified Takagi-Sugeno rule scheme. *Information Sciences* 123: 281-293.

Jaschke J, Yang X and Biegler LT (2014) Fast economic model predictive control based on NLP-sensitivities. *Journal of Process Control* 24:1260-1272.

Ji DH, Park JH, Yoo WJ and Won SC (2009) Robust memory state feedback model predictive control for discrete-time uncertain state delayed systems. *Applied Mathematics and Computation* 215: 2035-2044.

Kishor N (2008) Nonlinear predictive control to track deviated power of an identified NNARX model of a hydro plant. *Expert Systems with Applications* 35: 1741-1751.

Kim JS, Yoon TW, Shim H and Seo JH (2008) Switching adaptive output feedback model predictive control for a class of input-constrained linear plants. *IET Control Theory Applications* 2: 573-582.

Kirches C, Wirsching L, Bock HG and Schloder JP (2012) Efficient direct multiple shooting for nonlinear model predictive control on long horizons. *Journal of process control* 22:540-550.

Kunisaki C, Makino H, Akiyama H, et al. (2008) Predictive factors for anastomotic leakage in the neck after retrosternal reconstruction for esophageal cancer. *Hepato-Gastroenterology* 55:98-102.

La HC, Potschka A and Bock HG (2017) Partial stability for nonlinear model predictive control. *Automatica* 78:14-19.

Li HH, Chen DY, Zhang H, Wang FF and Ba DD (2016) Nonlinear modeling and dynamic analysis of a hydro-turbine governing system in the process of sudden load increase transient. *Mechanical Systems and Signal Processing* 80: 414-428.

Li HH, Chen DY, Zhang H, Wu CZ and Wang XY (2017) Hamiltonian analysis of a hydro-energy generation system in the transient of sudden load increasing. *Applied Energy* 185: 244-253.

Liu XJ, Kong XB and Lee KY (2016) Distributed model predictive control for load frequency control with dynamic fuzzy value position modelling for hydro-thermal power system. *IET Control Theory Applications* 10: 1653-1664.

Lam HK (2009) Stability analysis of T-S fuzzy control systems using parameter-dependent Lyapunov function. *IET Control Theory Applications* 3: 750-762.

Lopez-Negrete R, D'Amato FJ, Biegler LT and Kumar A (2013) Fast nonlinear model predictive control: Formulation and industrial process applications. *Computers & Chemical Engineering* 51:55-64.

Mobayen S and Tchier F (2017) Synchronization of a class of uncertain chaotic systems with Lipschitz nonlinearities using state-feedback control design: A matrix inequality approach. *Nonlinear Dynamics* 20: 1-15.

Mobayen S and Tchier F (2017) Composite nonlinear feedback control technique for master/slave synchronization of nonlinear systems. *Nonlinear Dynamics* 87: 1713-1747.

Mobayen S (2016) Optimal LMI-based state feedback stabilizer for uncertain nonlinear systems with time-varying uncertainties and disturbances. *Complexity* 21: 356-362.

Mobayen S (2015) An LMI-based robust for uncertain linear systems multiple time-varying delays using optimal composite nonlinear feedback technique. *Nonlinear Dynamics* 80: 917-927.

Mobayen S (2014) Robust tracking controller for multivariable delayed systems with input saturation via composite nonlinear feedback. *Nonlinear Dynamics* 76:827-838.

Mahmoud M, Dutton K and Denman M (2005) Design and simulation of a nonlinear fuzzy controller for a hydropower plant. *Electric Power Systems Research* 73: 87-99.

Martinez-Lucas G, Sarasua JI, Sanchez-Fernandez JA and Wilhelmi JR (2015) Power-frequency control of hydropower plants with long penstocks in isolated systems with wind generation. *Renewable Energy* 83: 245-255.

Munoz-Hernandez GA, Gracios-Marin CA, Jones DI, Mansoor SP, Guerrero-Castellanos JF and Portilla-Flores EA (2015) Evaluation of gain scheduled predictive control in a nonlinear MIMO model of a hydropower station. *International Journal of Electrical Power & energy Systems* 66: 125-132.

Moon UC and Lee KY (2009) Step-response model development for dynamic matrix control of a drum-type boiler-turbine system. *IEEE Transactions on Energy Conversion* 24: 423-430.

Ntogramatzidis L and Ferrante A (2011) Exact tuning of PID controllers in control feedback design. *IET Control Theory Applications* 5: 565-578.

Otsuka S, Uono S, Yoshimura S, Zhao S and Toichi M (2017) Emotion perception mediates the Predictive relationship between verbal ability and functional outcome in High-functioning adults with autism spectrum disorder. *Journal of Autism and Developmental Disorders* 47:1166-1182.

Rastegar S, Araujo R and Mendes J (2016) A new approach for online T-S fuzzy identification and model predictive control of nonlinear systems. *Journal of Vibration Control* doi:10.1177/1077546314544894.

Su BL, Chen ZQ and Yuan ZZ (2007) Constrained predictive control based on T-S fuzzy model for nonlinear systems. *Journal of Systems Engineering and Electronics* 18: 95-100.

Takacs G and Rohal'-llkiv B (2014) Model predictive control algorithms for active vibration control: a study on timing, performance and implementation properties.

*Journal of Vibration Control* doi:10.1177/107754631479993.

Tran QN, Ozkan L and Backx ACPM (2015) Generalized predictive control tuning by controller matching. *Journal of Process Contr*trol 25: 1-18.

Wang B, Xue JY and Chen DY (2016) Takagi -Sugeno fuzzy control for a wide class of fractional-order chaotic systems with uncertain parameters via linear matrix inequality. *Journal of Vibration Control* doi:10.1177/1077546314546682.

Wu S, Zhang RD, Lu RD and Gao FR (2014) Design of dynamic matrix control based PID for residual oil outlet temperature in a coke furnace. *Chemometrics and Intelligent Laboratory systems* 134: 110-117.

Xu BB, Chen DY, Zhang H and Zhou R (2015) Dynamic analysis and modeling of a novel fractional-order hydro-turbine-generator unit. *Nonlinear Dynamics* 81: 1263-1274.

Xu BB, Wang FF, Chen DY and Zhang H (2016) Hamiltonian modeling of multi-hydro-turbine governing systems with sharing common penstock and dynamic analyses under shock load. *Energy Conversion and Management* 108: 478-487.

Zhang H, Chen DY, Xu BB, et al. (2015) Nonlinear modeling and dynamic analysis of hydro-turbine governing system in the process of load rejection transient. *Energy Conversion and Management* 90: 128-137.

Zhang XY and Zhang MG (2006) An adaptive fuzzy PID control of hydro-turbine governor. *5th International Conference on Machine Learning and Cybernetics*, Dalian, China.

Zhang RF, Chen DY and Ma XY (2015) Nonlinear predictive control of a hydropower system model. *Entropy* 17: 6129-6149.

Zambelli MS, Lopes MS and Soares S (2012) Long-term hydropower scheduling using model predictive control approach with hybrid monthly-annual inflow forecasting. *6th IEEE/PES Transmission and Distribution - Latin America Conference and Exposition*, Montevideo, Urugay.

Zhang WY, Huang DX, Wang YD et al. (2008) Adaptive state feedback predictive control and expert control for a delayed coking furnace. *Chinese Journal of Chemical Eng*ineering 16: 590-598.

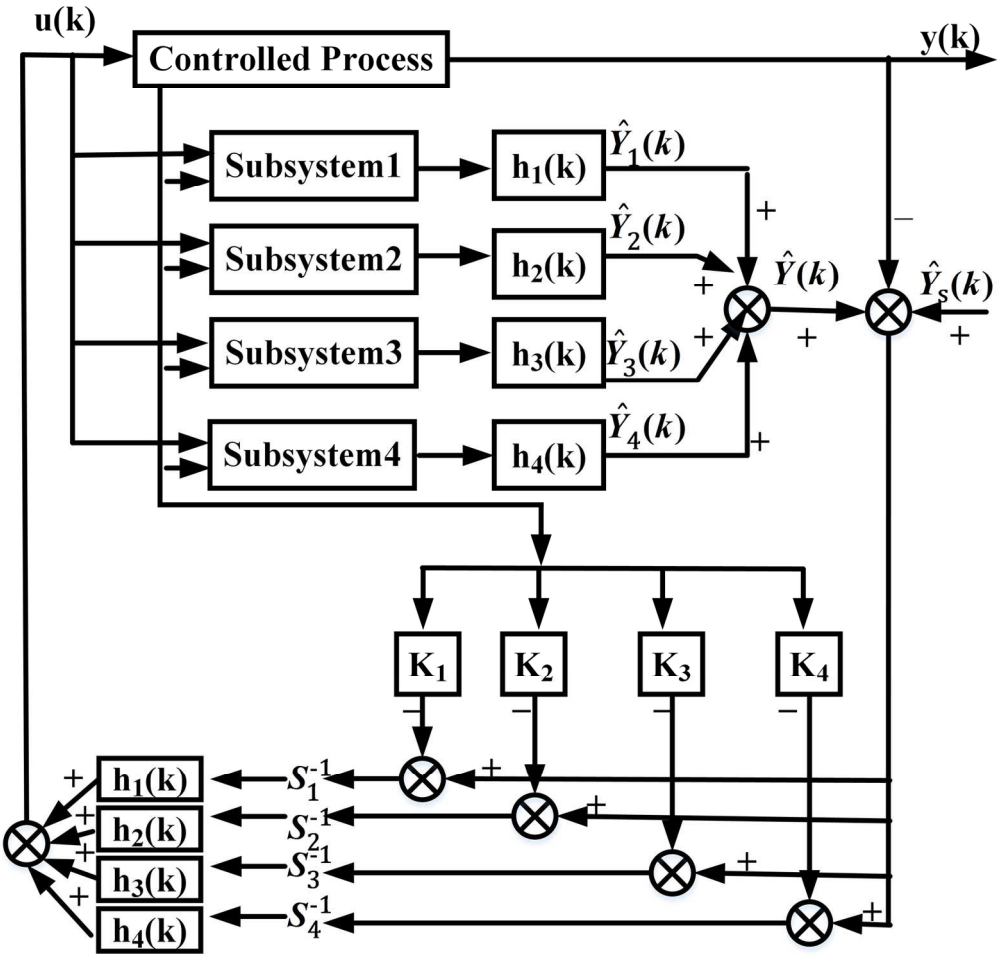


156x152mm (300 x 300 DPI)

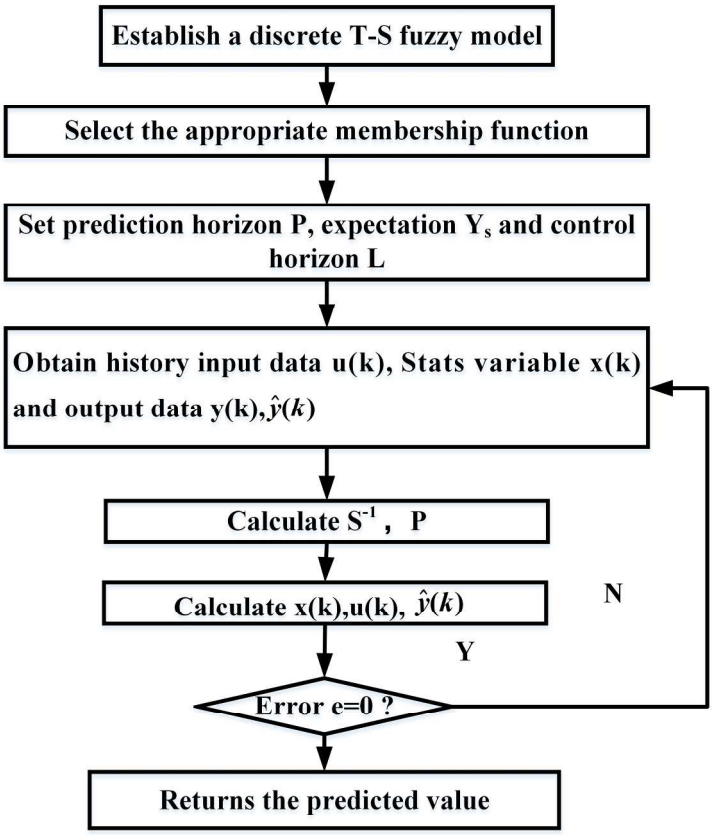


225x251mm (300 x 300 DPI)

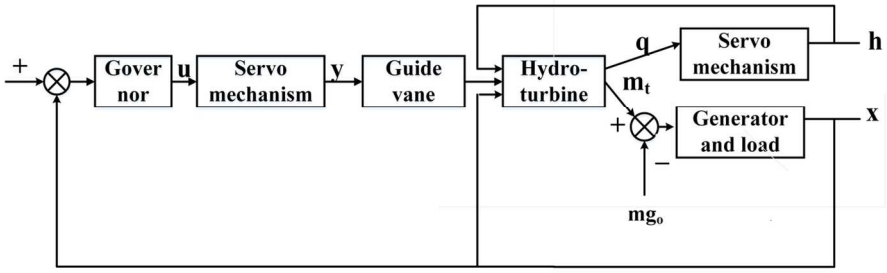


130x43mm (300 x 300 DPI)

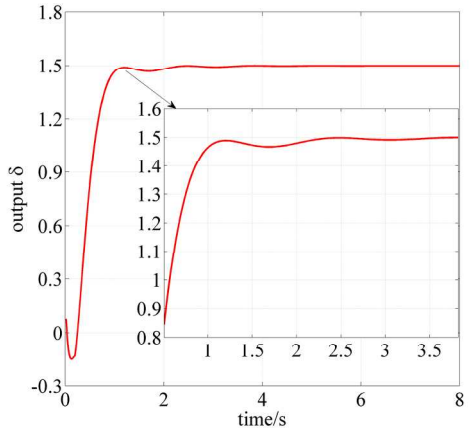


194x89mm (300 x 300 DPI)

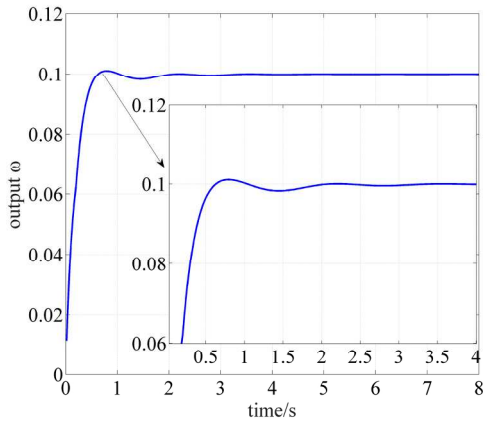


194x89mm (300 x 300 DPI)

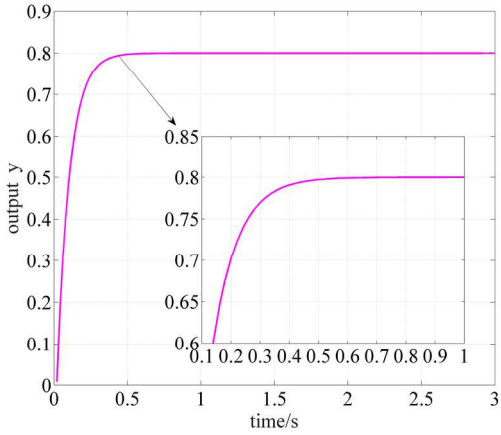


194x89mm (300 x 300 DPI)

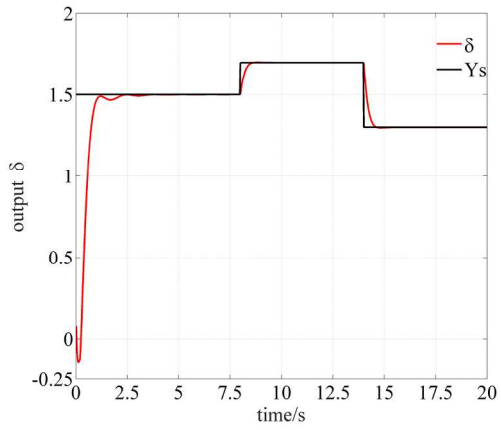


194x89mm (300 x 300 DPI)

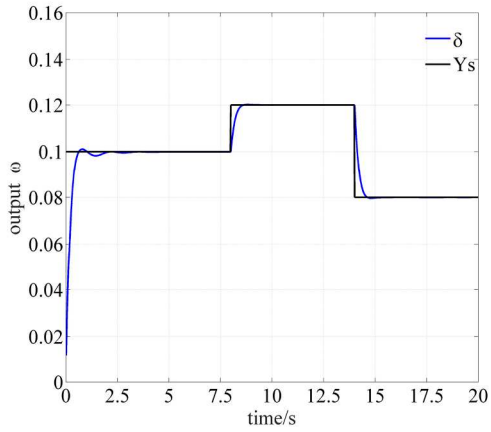


194x89mm (300 x 300 DPI)

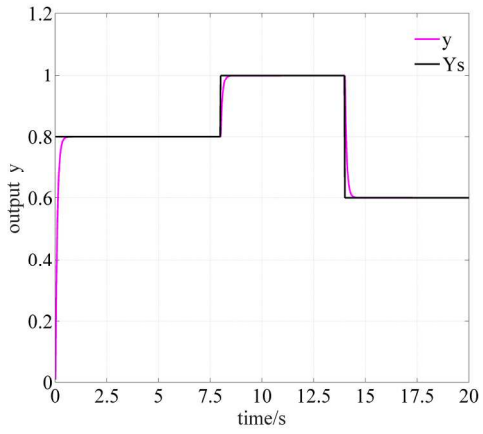


194x89mm (300 x 300 DPI)

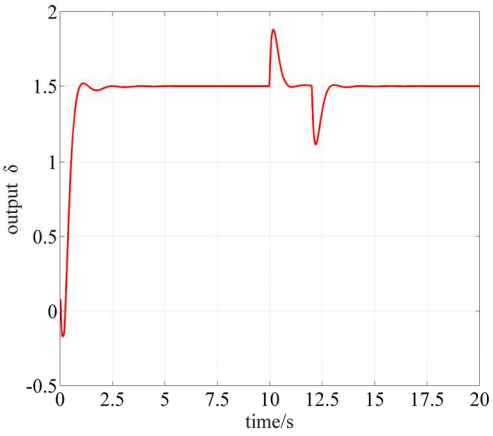


194x89mm (300 x 300 DPI)

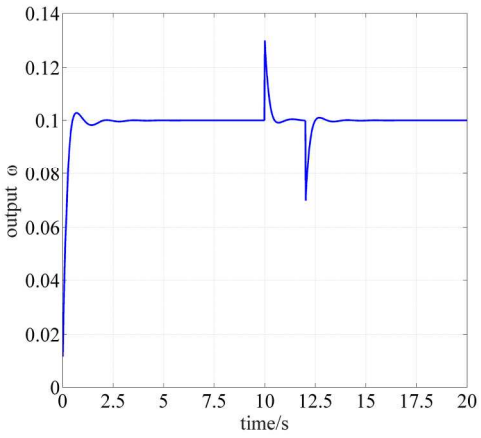


194x89mm (300 x 300 DPI)

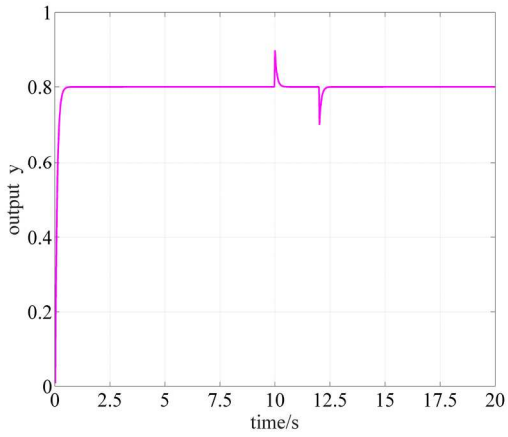


194x89mm (300 x 300 DPI)

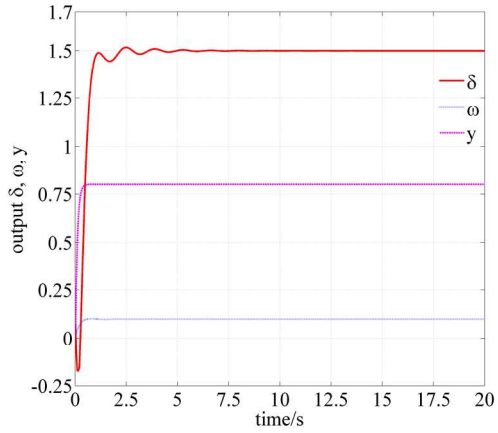


194x89mm (300 x 300 DPI)

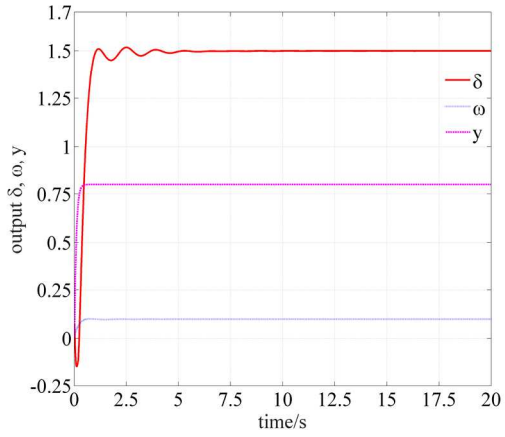


194x89mm (300 x 300 DPI)

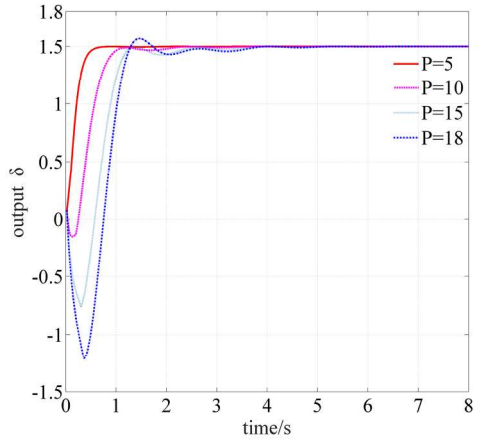


194x89mm (300 x 300 DPI)

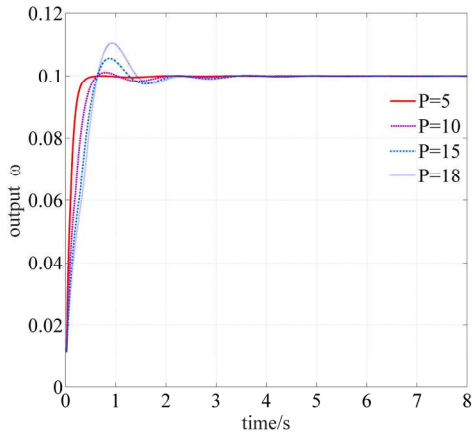


194x89mm (300 x 300 DPI)

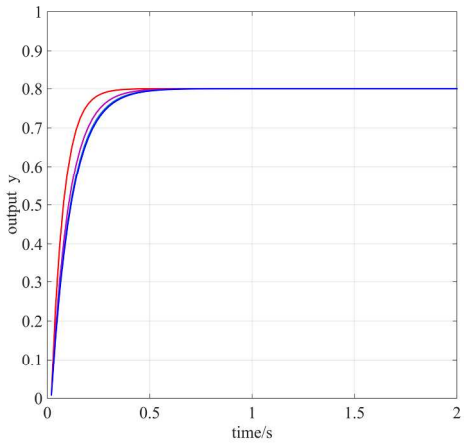


241x114mm (300 x 300 DPI)

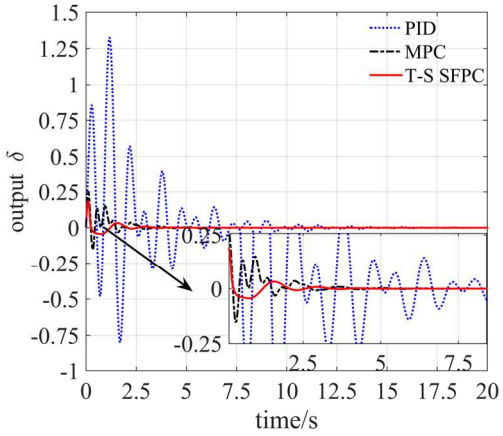


159x69mm (300 x 300 DPI)

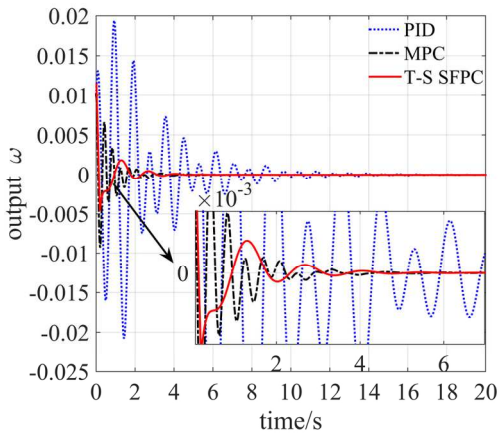


159x69mm (300 x 300 DPI)

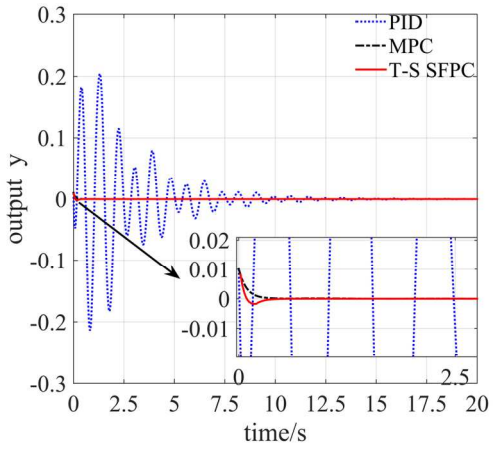


159x69mm (300 x 300 DPI)

**Table 1** Adjusting time of the HTGS under MPC, PID and T-S SFPC controllers

| | $\delta$ | | | $\omega$ | | | $y$ | | |
|---|---|---|---|---|---|---|---|---|---|
| | PID | MPC | T-S SFPC | PID | MPC | T-S SFPC | PID | MPC | T-S SFPC |
| T/s | 16.6 | 4.8 | 3.6 | 16.1 | 5.8 | 4.5 | 16.5 | 0.5 | 0.5 |